

Electron-impact excitation of the $3s3p\ ^1P_1$ state of magnesium: Electron scattering at small angles

D.M. Filipović^{a,b}, B. Predojević^{a,1}, D. Šević^a, V. Pejčev^a, B.P. Marinković^{a,*},
Rajesh Srivastava^c, A.D. Stauffer^d

^a Institute of Physics, Belgrade, P.O. Box 68, 11080 Belgrade, Serbia and Montenegro

^b Faculty of Physics, University of Belgrade, P.O. Box 368, 11001 Belgrade,
Serbia and Montenegro

^c Department of Physics, Indian Institute of Technology, Roorkee 247667, India

^d Department of Physics and Astronomy, York University, Toronto, Canada M3J 1P3

Received 28 December 2005; received in revised form 13 January 2006; accepted 16 January 2006

Available online 17 February 2006

Abstract

Absolute differential cross sections for electron-impact excitation of the $3s3p\ ^1P_1$ state in magnesium at incident electron energies of $E_0 = 10, 13, 15, 20, 40, 60, 80$ and 100 eV have been experimentally derived and corresponding calculations have been carried out. The measurements are performed at small scattering angles from 2° to 14° . The forward scattering function method has been used for determination of the absolute values, except at $E_0 \leq 15$ eV where the excitation function of the $3s3p\ ^1P_1$ state experimentally obtained by [D. Leep, A. Gallagher, Phys. Rev. A 13 (1976) 148] was utilized for normalization. The calculations have been performed in the relativistic distorted-wave approximation. The results are analyzed and compared with other available experimental data and theoretical calculations.

© 2006 Elsevier B.V. All rights reserved.

PACS: 34.80.Dp

Keywords: Magnesium; Electron excitation; Differential cross section

1. Introduction

Magnesium is a “light” earth-alkaline atom ($Z = 12$) with two $3s$ valence electrons in the ground state. This electronic structure of the outer shell is the same as in ytterbium ($Z = 70$), which has been investigated experimentally in our laboratory recently by Predojević et al. [1,2]. In this work we focus our attention on the quantities that may depend on the atomic number at intermediate incident electron energies, $E_0 = 10$ – 100 eV. An important quantity in this sense is the differential cross section (DCS) at small scattering angles for dipole-allowed transitions.

There are a few papers with experimental investigations of electron interactions with magnesium vapours. Williams and

Trajmar [3] measured cross sections for elastic scattering and several excitations including the resonance transition at impact energies of $10, 20$ and 40 eV. At the same electron-impact energies, Brunger et al. [4] determined DCSs for the $3s3p\ ^1P_1$ state in the angular range from 5° to 130° at energies of 10 and 20 eV and from 3° to 130° at 40 eV in 1° steps at small angles. More recently, Brown et al. have studied the $3s3p\ (^1P_1$ and $^3P_1)$ states by using the polarized-photon–scattered-electron correlation method and they have obtained the DCS at 40 eV [5] and 20 eV [6] impact energies.

Several calculations of DCSs for inelastic electron scattering by magnesium have been performed. Fabrikant [7] calculated DCSs for the $3s^2\ ^1S \rightarrow 3s3p\ ^1P$ transition at incident electron energies of 10 and 20 eV using the two-state close-coupling (CC2) approximation. Mitroy and McCarthy [8] computed DCSs for the elastic scattering and excitation of the four lowest singlet states ($3s3p\ ^1P_1, 3s4s\ ^1S_0, 3s4d\ ^1D_2$ and $3s4p\ ^1P_1$) at $E_0 = 10, 20, 40$ and 100 eV using the five-state close-coupling (CC5) calculation. McCarthy et al. [9] calcu-

* Corresponding author. Tel.: +381 11 316 0882; fax: +381 11 316 2190.

E-mail address: bratislav.marinkovic@phy.bg.ac.yu (B.P. Marinković).

¹ Permanent address: Faculty of Natural Sciences, University of Banja Luka, Republic of Srpska, Bosnia and Herzegovina.

lated DCSs for the elastic and inelastic (excitation of the $3s3p\ ^1P_1$ and 3P_1 states) scattering at $E_0 = 10, 20$ and 40 eV using the six-state close-coupling (CC6 and optical CCO6) methods. Meneses et al. [10] used the first-order many-body theory (FOMBT) to calculate DCSs for excitation of the $3s3p$ (1P_1 and 3P_1) states at $E_0 = 20, 30, 40, 50$ and 100 eV. Clark et al. [11] used both the FOMBT and distorted-wave approximation (DWA) for calculations of DCSs for the $3s3p\ ^1P_1$ state at 10 and 40 eV. Kaur et al. [12] used the relativistic distorted-wave approximation (RDW) for calculation of DCSs for the $3s3p$ (1P_1 and $^3P_{0,1,2}$), $3s3d$ (1D_2 and $^3D_{1,2,3}$) and $3s4p$ (1P_1 and $^3P_{0,1,2}$) states in magnesium at $E_0 = 10, 20$ and 40 eV. Fursa and Bray [13] calculated DCSs for electron-impact excitation of the $3s3p\ ^1P_1$ state at $E_0 = 10, 20$ and 40 eV using the 27-state and convergent close-coupling (CC27 and CCC) approach.

We report generalized oscillator strengths (GOSs) for the $3s^2\ ^1S_0 \rightarrow 3s3p\ ^1P_1$ transition as well as DCSs for electron-impact excitation of the $3s3p\ ^1P_1$ state of magnesium at $E_0 = 10, 13, 15, 20, 40, 60, 80$ and 100 eV and small scattering angles from 2° to 14° . In Section 2, the experimental set-up is described and the experimental procedure is given. In Section 3, the RDW method as applied to the calculation of the differential cross section calculation is outlined. In Section 4, figures for the generalized oscillator strengths are shown and absolute DCS values are tabulated and presented graphically. Finally, in Section 5, our results are discussed and compared with previous measurements and calculations.

2. Apparatus and experimental procedure

The apparatus used is a conventional crossed-beam electron spectrometer described in more detail in our recent paper dealing with electron scattering by zinc (Panajotović et al. [14]). The present electron spectrometer can be operated in three different modes: recording of electron energy-loss spectra, scanning incident energy and direct angular distribution measuring of elastically and inelastically scattered electrons. A channel electron multiplier is utilized for single-electron counting. The analyzer can be positioned from -30° up to $+150^\circ$. The real zero scattering angle was determined on the basis of symmetry of the inelastically (excitation of the $3s3p\ ^1P_1$) scattered electron intensity with respect to the mechanical zero, within 0.2° uncertainty. The angular resolution of the spectrometer is estimated to be 1.5° (2° at 10 eV because of spreading of the low energy electron beam produced by the monochromator). Overall system energy resolution (FWHM) of about 120 meV was maintained for these measurements. The energy scale was calibrated against the $3s3p\ ^1P_1$ excitation threshold of Mg at 4.346 eV. Using significantly improved energy resolution (50 meV), we did not find the shift of the energy scale due to contact potential difference between the thoriated tungsten filament (work function of Th is 3.4 eV) and the magnesium plated (3.66 eV) collision chamber. The uncertainty in the energy was estimated to be less than 0.1 eV.

Construction of the oven for the metal vapour, which was used as well for producing and controlling the vapour beam was the same as in the case of ytterbium [1,2]. The measurements were performed at a temperature of 780 K for magnesium of 99.9% purity. At this temperature, the number density of the magnesium effusing through the cylindrical channel (aspect ratio $\gamma = 0.075$) from the crucible was 10^{13} to 10^{14} cm^{-3} in the interaction volume. Water cooling of the oven shield protected the channel electron multiplier from a rise in temperature during long term measurements.

Relative DCSs for the $3s3p\ ^1P_1$ state were obtained by direct angular distribution measurements. Briefly, for a given E_0 , the position of the analyzer was changed around mechanical zero from -10° to approximately 15° and the angular distribution of scattered electrons was measured. To obtain relative DCSs a correction of the scattering intensity was made using the effective path-length correction factors according to the approach of Brinkman and Trajmar [15].

In the present work we have used the forward scattering function (FSF) method introduced by Avdonina et al. [16] for determination of the absolute DCS values. The FSF curve was obtained using the experimental optical oscillator strength (OOS) of 1.83 ± 0.08 by Liljeby et al. [17].

Contributions to the total error of the absolute DCSs come from: (a) uncertainties in our experimental values and (b) uncertainty in the normalization procedure. The errors in our experimental values arise from statistical errors, uncertainty of the effective path-length correction factor (0.06) and estimation of the energy (0.01) and angular (0.10) scales mentioned above. Uncertainty in the normalization procedure (0.10) arises from uncertainty of the OOS (0.04) and fitting of the relative GOSs. Overall uncertainty of our experimental DCS values is below 0.16 , except at 10 eV impact energy where the overall uncertainty is below 0.20 .

3. Calculation method

In our previous calculations on magnesium (Kaur et al. [12]) we used simple target state wave functions involving only the spectroscopic orbitals. However, our recent calculations on calcium (Chauhan et al. [18]) indicated the importance of having good quality target wave functions in order to obtain accurate DCSs. Thus we have performed an elaborate configuration interaction Dirac Fock calculation using the GRASP92 program of Parpia et al. [19].

In the relativistic $j-j$ coupling notation, the ground 1S_0 state configurations of magnesium is $1s^2 2s^2 2\bar{p}^2 2p^4 3s^2$ where \bar{p} and p indicate p-electrons with total angular momenta j of $1/2$ and $3/2$, respectively. The excited 1P_1 state is a linear combination of the $3s3\bar{p}$ and $3s3p$ valence configurations. In our configuration interaction calculations we have added to these basic spectroscopic configurations the valence configurations $3s4s$, $3\bar{p}^2$, $3\bar{p}4\bar{p}$, $3p^2$, $3p4p$, $3\bar{d}^2$ and $3d^2$ in the ground state and the valence configurations $3s4\bar{p}$, $3s4p$, $3\bar{p}3\bar{d}$, $3\bar{p}4s$, $3\bar{p}3d$, $3p3d$ and $3p4s$ in the excited state. This yielded an energy for the 1P_1 state of 4.341 eV and an oscillator strength for the transition from ground to excited

state of 1.77. Both of these values are in excellent agreement with the experimentally determined ones.

The distorted-wave T-matrix for the electron-impact excitation of an atom having N electrons and nuclear charge Z from an initial state i to final state f can be written as [20] (atomic units are used throughout)

$$T_{i \rightarrow f}^{\text{DW}} = \langle \chi_f^-(1, 2, \dots, N+1) | V - U_f(N+1) | A \chi_i^+(1, 2, \dots, N+1) \rangle \quad (1)$$

where V is the target–projectile interaction given by

$$V = -\frac{Z}{r_{N+1}} + \sum_{j=1}^N \frac{1}{|\mathbf{r}_j - \mathbf{r}_{N+1}|}. \quad (2)$$

Here \mathbf{r}_j ($j = 1, \dots, N$) represents the position co-ordinates of the target electrons and \mathbf{r}_{N+1} is the position co-ordinate of the projectile electron with respect to the nucleus of the atom. U_f is the distortion potential which is taken to be a function of the radial co-ordinates of the projectile electron only, i.e., r_{N+1} . Also U_f is chosen to be a spherically averaged static potential of the excited state of atoms. This choice of U_f has been shown to yield most consistent results [21].

The wave functions $\chi_{\text{ch}}^{+(-)}$, where ‘ch’ refers to the two channels, i.e., initial ‘i’ and final ‘f’, are represented as a product of the N -electron target wave functions ϕ_{ch} as detailed above and a projectile electron distorted-wave function $F_{i(f)}^{\text{DW}+(-)}$, i.e.,

$$\chi_{\text{ch}}^{+(-)}(1, 2, \dots, N+1) = \phi_{\text{ch}}(1, 2, \dots, N) F_{i(f)}^{\text{DW}+(-)}(\mathbf{k}_{\text{ch}}, N+1). \quad (3)$$

Here ‘+’ refers to an outgoing wave while ‘–’ denotes an incoming wave. A is the antisymmetrization operator that takes into account the exchange of the projectile electron with the target electrons and \mathbf{k}_{ch} are the linear momenta of the projectile electron in the initial and final state. The method of calculating the distorted waves was given in [12].

We define the scattering amplitude for the excitation of the 3^1P_1 state with magnetic quantum number M as

$$f(M, \mu_f, \mu_i) = (2\pi)^2 \sqrt{\frac{k_f}{k_i}} T_{i \rightarrow f}^{\text{DW}}(M, \mu_f, \mu_i) \quad (4)$$

where μ_i and μ_f are the spin projections in the initial and final channels. Then with our normalization the DCS is given by

$$\text{DCS} = \frac{1}{2} \sum_{M, \mu_i, \mu_f} |f(M, \mu_i, \mu_f)|^2. \quad (5)$$

4. Results

We have measured relative differential cross sections for electron-impact excitation of the $3s3p^1P_1$ state in magnesium at incident electron energies of 10, 13, 15, 20, 40, 60, 80 and 100 eV. The normalized-to-relative GOS quotients have been

used as normalization factors for putting our relative DCSs on the absolute scale at 20, 40, 60, 80 and 100 eV. Relative DCSs at 10, 13 and 15 eV have been normalized to the excitation function of the $3s3p^1P_1$ state experimentally obtained by Leep and Gallagher [22]. The reason for using two different normalization procedures is discussed in the next section. Normalized generalized oscillator strengths for the excitation of the $3s3p^1P_1$ versus the squared momentum transfer (K^2) and their linear fits at all energies that we have studied are plotted in Fig. 1(a) and (b). Present experimental and theoretical GOSs at $E_0 = 10, 20$ and 40 eV are shown in Fig. 2, together with those experimentally obtained by Brunger et al. [4] and calculated by Mitroy and McCarthy [8] and Fursa and Bray [13]. In addition, the FSF and our calculated GOSs, together with our representative GOS at a single energy of 60 eV are shown in Fig. 3.

The present experimental DCSs for electron-impact excitation of the $3s3p^1P_1$ state at $E_0 = 10, 13, 15, 20, 40, 60, 80$, and 100 eV are given in Table 1. These DCSs with total errors as determined in the manner described above are presented in Figs. 4 and 5. The present calculations are presented as well. In the same figures the measured DCSs by Brunger et al. [4] and Williams and Trajmar [3] (only at 10°) are presented as well as

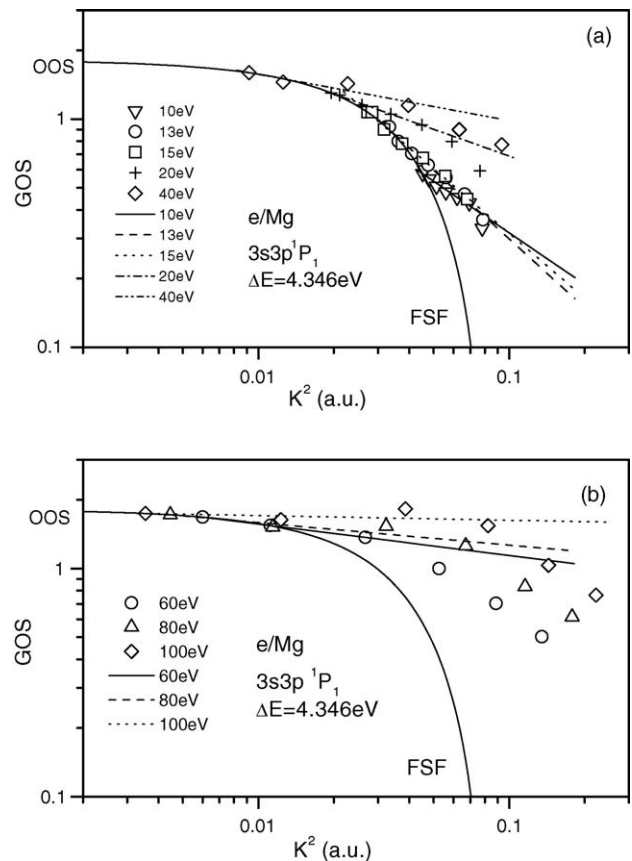


Fig. 1. Generalized oscillator strengths (GOS) for electron-impact excitation of the $3s3p^1P_1$ state of Mg atom (energy-loss $\Delta E = 4.346$ eV) at: (a) 10, 13, 15, 20 and 40 eV; (b) 60, 80 and 100 eV incident electron energies. FSF is the forward scattering function. The straight lines are linear fits to the measured data. The optical oscillator strength $\text{OOS} = 1.83 \pm 0.08$ by Liljeby et al. [17] is adopted.

Table 1

Differential cross sections (in units of $10^{-20} \text{ m}^2 \text{ sr}^{-1}$) for electron-impact excitation of the $3s3p \ ^1P_1$ state of the Mg atom

Angle ($^\circ$)	10 (eV)	13 (eV)	15 (eV)	20 (eV)	40 (eV)	60 (eV)	80 (eV)	100 (eV)
2	51.4	113	148	186	382	465	426	537
4	44.9	90.1	111	138	207	173	152	151
6	38.9	70.5	81.7	96.3	95.7	64.1	60.0	49.7
8	33.7	54.0	58.3	65.1	46.9	26.7	23.1	18.4
10	28.8	40.3	39.8	41.8	27.3	12.6	11.0	6.79
12	24.4	28.8	25.8	24.1				
14	16.8	18.8						

the CC5 and CCC calculations by Mitroy and McCarthy [8] and Fursa and Bray [13].

5. Discussion and conclusion

The high angular resolution of our spectrometer makes the measurement of DCSs at small scattering angles possible. However, it is not possible to measure the DCSs at angles $\theta < 2^\circ$ because of the following reasons: (a) the influence of the primary beam near 0° and (b) the angular resolution of 1.5° and

uncertainty of the zero position of 0.2° that limits our measurements of strongly forward peaked angular distributions to 2° .

It is important to know accurately both the energy dependence and small scattering angle behavior of a relative DCS curve if the normalization procedure is to be based on these data. The FSF method may not be used for normalization of the relative DCS at $E_0 = 10 \text{ eV}$ because the necessary condition $E_0 \geq 2.5\omega$ (where $\omega = 4.346 \text{ eV}$ is the excitation energy) is not satisfied. At energies close to this limit ($E_0 \leq 15 \text{ eV}$) we normalized our experimental DCSs to the optical excitation function measured by Leap

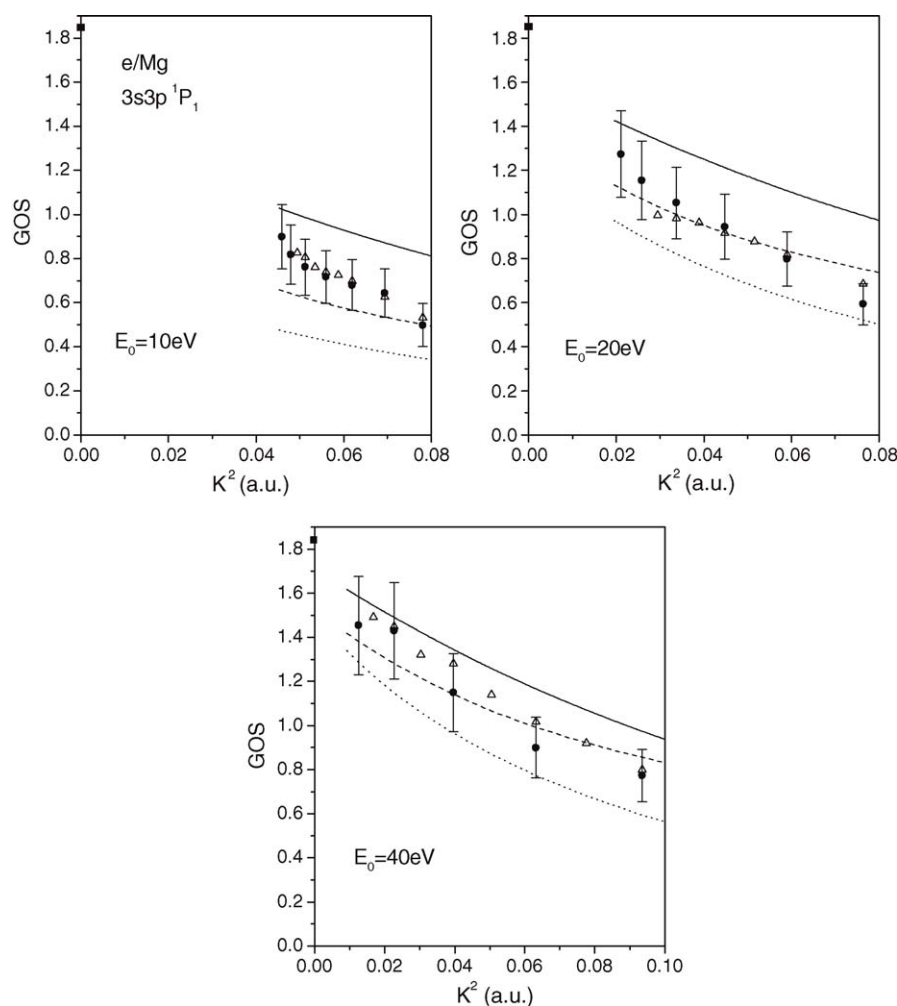


Fig. 2. Generalized oscillator strengths (GOS) for electron-impact excitation of the $3s3p \ ^1P_1$ state of Mg atom at 10, 20 and 40 eV incident electron energies. (●) Present experiment (total error bars are indicated); (—) present RDW calculation; (Δ) Brunger et al. [4]; (---) CC5 (Mitroy and McCarthy [8]); (···) CCC (Fursa and Bray [13]); (■) the optical oscillator strength.

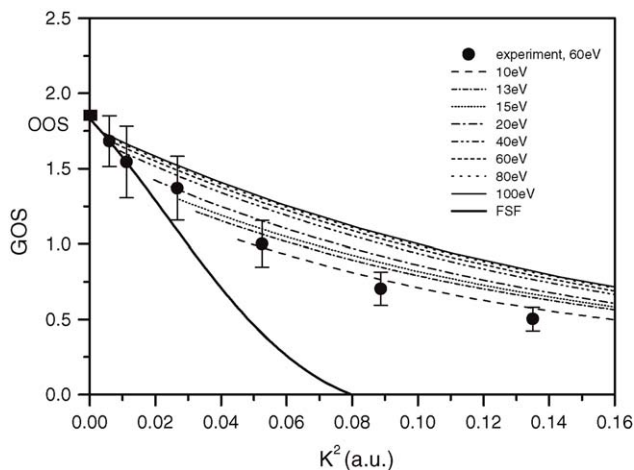


Fig. 3. Generalized oscillator strengths (GOS) for electron-impact excitation of the $3s3p\ ^1P_1$ state of Mg atom. The present RDW calculations at all incident energies and the experimentally obtained GOS at 60 eV incident electron energy are shown. FSF and OOS (■) are the forward scattering function and optical oscillator strength, respectively.

and Gallagher [22]. If the FSF method is applied to the relative DCSs at $E_0 = 13$ and 15 eV, then the absolute DCSs are smaller by approximately 30% and 25%, respectively, when compared to the corresponding experimental DCSs reported here. This indicates the difficulty of the normalization of experimental data at low energies and small scattering angles. These uncertainties are twice as large of our claimed uncertainties at these low energies. For the normalization of our relative experimental DCSs at $E_0 \geq 20$ eV we have used the FSF method as the universal one, based on the accurate OOS value. As usual, the intervals of linearity of the $\log(\text{GOS})$ versus $\log(K^2)$ function and the slopes of corresponding linear fits become smaller with the increase of the incident electron energy (Fig. 1).

One can see in Fig. 2, a good agreement between present experimental GOSs and those by Brunger et al. [4]. The agreement among the various calculations is not as good. As shown in Fig. 3, where linear scale for K^2 is used, our calculated GOSs at corresponding $(K^2)_{\text{min}}$ are in better agreement with the FSF curve as the energy increases.

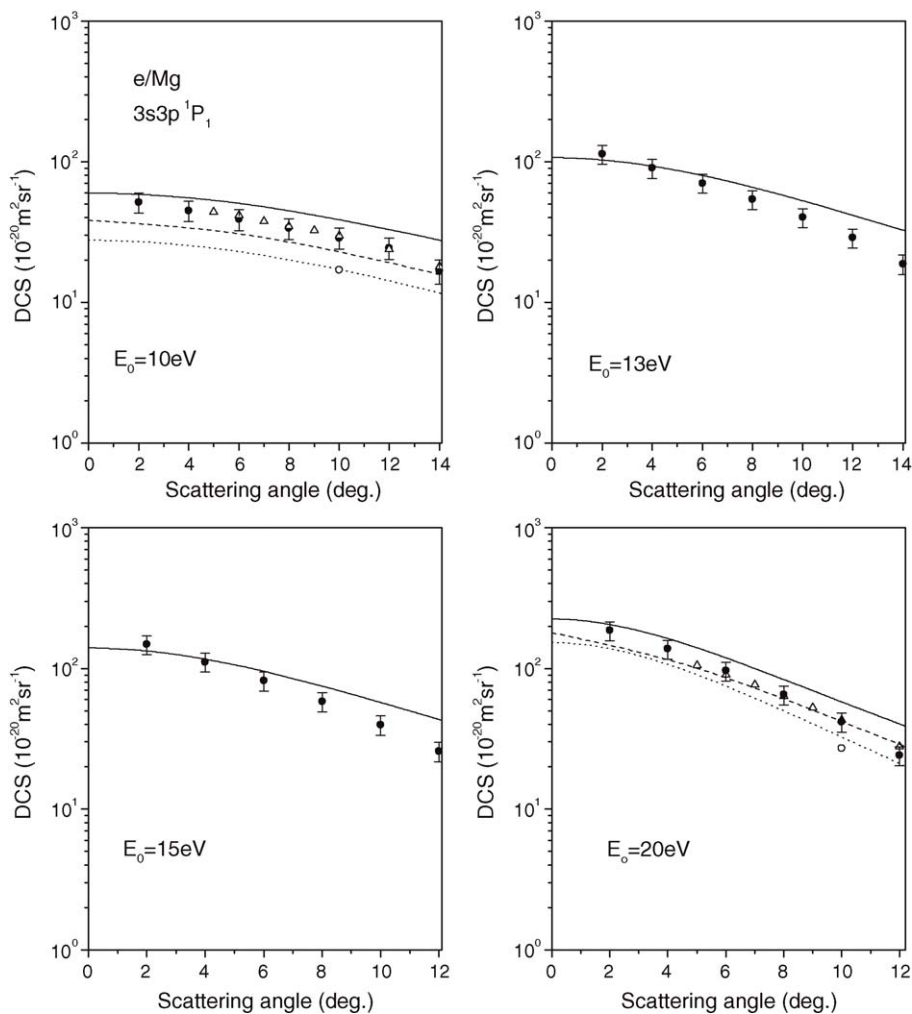


Fig. 4. Differential cross sections (DCS) for electron-impact excitation of the $3s3p\ ^1P_1$ state of Mg atom at: 10, 13, 15, and 20 eV impact energies. (●) Present experiment (total error bars are indicated); (—) present RDW calculation; (Δ) Brunger et al. [4]; (\circ) Williams and Trajmar [3]; (---) CC5 (Mitroy and McCarthy [8]); (-·-) CCC (Fursa and Bray [13]).

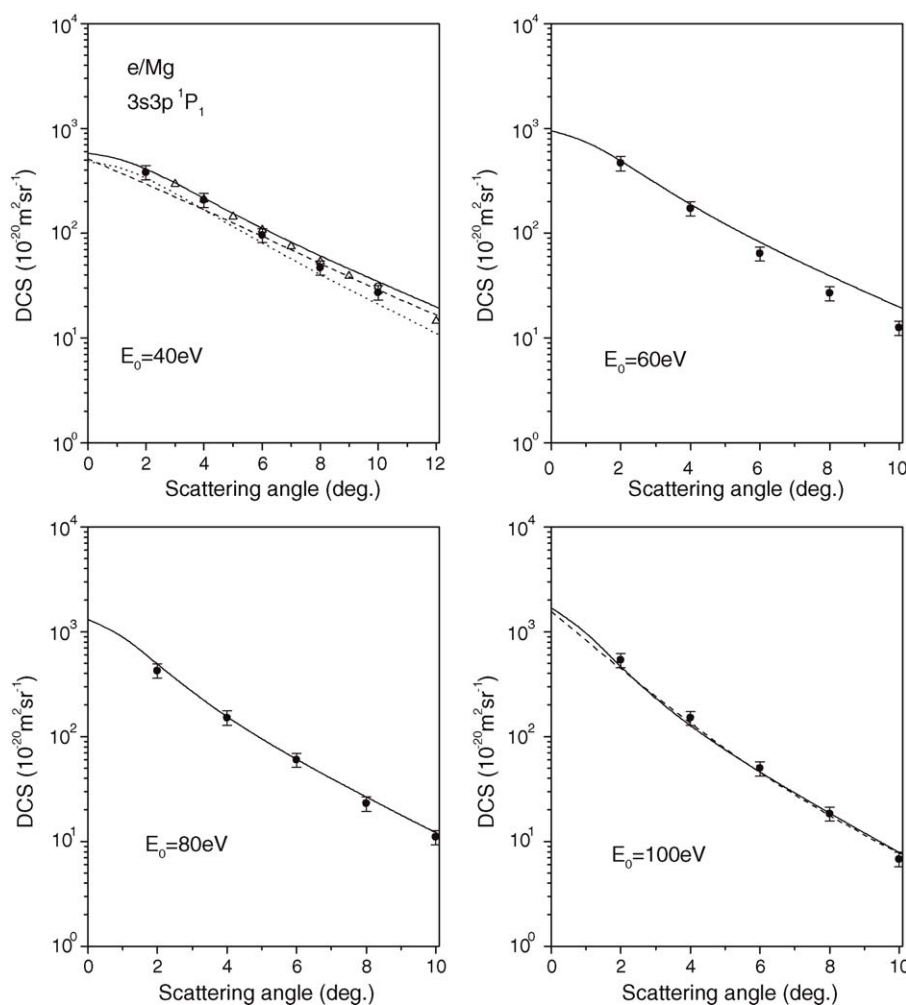


Fig. 5. Same as Fig. 4, but at 40, 60, 80 and 100 eV incident electron energies.

A good agreement between our experimental DCSs and those measured by Brunger et al. [4] is clearly seen in Figs. 4 and 5. The DCSs at 10° scattering angle measured by Williams and Trajmar [3] (the errors are not given) are lower than ours by approximately 40% at $E_0 = 10$ and 20 eV, but higher by approximately 10% at 40 eV. A general conclusion from Figs. 4 and 5 is that the other theories predict lower DCS values than those experimentally obtained at small scattering angles but the agreement improves as the scattering angle increases. The agreement between our experimental DCSs and our RDW calculation is excellent at scattering angles below 5° . At higher angles the agreement is very good especially at higher impact energies (80 and 100 eV) where the agreement is within experimental error bars in the domain of scattering angles considered. But, a little and systematic drop of measured data compared with calculated ones could be noticed. Extension of DCSs to higher scattering angles is a challenge for both experiment and theory.

Acknowledgements

We thank Dr. D. Fursa for sending us his calculated e/Mg data in numerical form. This experimental work has been carried out within MNZZS project no. 141011 of Republic of Serbia. The

theoretical calculations were supported by the Natural Sciences and Engineering Research Council of Canada.

References

- [1] B. Predojević, D. Šević, V. Pejčev, B.P. Marinković, D.M. Filipović, J. Phys. B: At. Mol. Opt. Phys. 38 (2005) 1329.
- [2] B. Predojević, D. Šević, V. Pejčev, B.P. Marinković, D.M. Filipović, J. Phys. B: At. Mol. Opt. Phys. 38 (2005) 3489.
- [3] W. Williams, S. Trajmar, J. Phys. B: At. Mol. Phys. 11 (1978) 2021.
- [4] M.J. Brunger, J.L. Riley, R.E. Scholten, P.J. Teubner, J. Phys. B: At. Mol. Opt. Phys. 21 (1988) 1639.
- [5] D.O. Brown, D. Cvejanović, A. Crowe, J. Phys. B: At. Mol. Opt. Phys. 36 (2003) 3411.
- [6] D.O. Brown, A. Crowe, D.V. Fursa, I. Bray, K. Bartschat, J. Phys. B: At. Mol. Opt. Phys. 38 (2005) 4123.
- [7] I.I. Fabrikant, J. Phys. B: At. Mol. Phys. 13 (1980) 603.
- [8] J. Mitroy, I.E. McCarthy, J. Phys. B: At. Mol. Opt. Phys. 22 (1989) 641.
- [9] I.E. McCarthy, K. Ratnavelu, Y. Zhou, J. Phys. B: At. Mol. Opt. Phys. 22 (1989) 2597.
- [10] G.D. Meneses, C.B. Pagan, L.E. Machado, Phys. Rev. A 41 (1990) 4740.
- [11] R.E.H. Clark, G. Csanak, J. Abdallah, Phys. Rev. A 44 (1991) 2874.
- [12] S. Kaur, R. Srivastava, R.P. McEachran, A.D. Stauffer, J. Phys. B: At. Mol. Opt. Phys. 30 (1997) 1027.
- [13] D.V. Fursa, I. Bray, Phys. Rev. A 63 (2001) 032708.

- [14] R. Panajotović, D. Šević, V. Pejčev, D.M. Filipović, B.P. Marinković, *Int. J. Mass. Spectrom.* 233 (2004) 253.
- [15] W. Brinkman, S. Trajmar, *J. Phys. E: Sci. Instrum.* 14 (1981) 245.
- [16] N.B. Avdonina, Z. Felfli, A. Msezane, *J. Phys. B: At. Mol. Opt. Phys.* 30 (1997) 2591.
- [17] L. Liljeby, A. Lindgard, S. Mannervik, E. Veje, B. Jelenković, *Phys. Scripta* 21 (1980) 805.
- [18] R.K. Chauhan, R. Srivastava, A.D. Stauffer, *J. Phys. B: At. Mol. Opt. Phys.* 38 (2005) 2385.
- [19] F.A. Parpia, C. Froese Fischer, I.P. Grant, *Comput. Phys. Commun.* 94 (1996) 249.
- [20] C.J. Joachain, *Quantum Collision Theory*, Amsterdam, North-Holland, 1983.
- [21] T. Zuo, Ph.D. Thesis, York University, Toronto, 1991.
- [22] D. Leep, A. Gallagher, *Phys. Rev. A* 13 (1976) 148.